

Shape anisotropy effect on magnetic domain wall dynamics in nanowires under thermal gradient

M. T. Islam^{a,*}, J. M. T. Islam^a, M. A. S. Akanda^a, M. A. J. Pikul^a and F. Yesmin^a

^aPhysics Discipline, Khulna University, Khulna 9208, Bangladesh

ARTICLE INFO

Keywords:

Domain wall dynamics
Thermal gradient
sLLG equation
Racetrack memory

ABSTRACT

We investigate the magnetic-domain wall (DW) dynamics in uniaxial/biaxial-nanowires under a thermal gradient (TG). The findings reveal that the DW propagates toward the hotter region in both nanowires. In uniaxial-nanowire, the DW propagates accompanying a rotation of the DW-plane. In biaxial nanowire, DW propagates in the hotter region, and the so-called Walker breakdown phenomenon is observed. The main physics of such DW dynamics is the magnonic angular momentum transfer to the DW. The hard (shape) anisotropy exists in biaxial-nanowire, which contributes an additional torque; hence DW speed is larger than that in uniaxial-nanowire. But rotational speed is lower initially as hard anisotropy suppresses the DW-rotation. After certain TG, DW-plane overcomes the hard anisotropy; thus, the rotational speed increases again. DW dynamics show a decreasing trend with the damping since the magnon propagation length decreases. Therefore, the above findings might be useful to realize the spintronics (i.e., fast racetrack memory) devices.

1. Introduction

Efficient manipulation of magnetic domain wall (DW) in nanostructures has drawn much attention because of its potential applications in spintronic devices such as in data storage devices [1] and logic operations [2]. Several controlling parameters, such as magnetic fields, microwaves, and spin-polarized currents, have been reported in the recent decade to drive DW in magnetic nanostructures. But these parameters suffer from certain limitations in applications. Particularly, in the case of magnetic-field driven, the DW propagation is obtained because of the energy dissipation [3, 4]. However, the magnetic field is unable to drive a series of DWs synchronously [5, 6, 7]. On the other hand, an electric current can drive a DW, or a series of DWs in the same direction with the mechanism of angular momentum transfer [8, 9, 10, 11]. Besides, a high critical current density is required to obtain a useful DW speed, which causes a Joule heating problem. [7, 12, 13]. To overcome such challenges, spin-wave-spin-current generated by thermal gradient (TG) emerges as an alternative driving force for the DW motion [14, 15]. Therefore, the study of TG-driven DW motion is significant not only for spintronic device applications but also for the understanding of the interplay between spin-wave and magnetic DW [16, 17].

Presently, to explain the physical picture of the TG driven DW dynamics, two theories of different origins are available, namely, microscopic (magnonic theory) theory [18, 19, 20, 21] and macroscopic (thermodynamic theory) theory [22, 23, 24]. The microscopic theory predicts that more magnons are generated in the hotter part and diffuse from the hotter to the colder part, and thus a magnonic spin current is produced. While magnons pass through the DW, magnons ex-


ert a magnonic torque on the DW by transferring spin angular momentum to the DW. Thus, magnons drive the DW toward the hotter region of the nanowire, opposite to the direction of the magnonic current [16, 19, 25]. The thermodynamic theory suggests that, in order to minimize the system free energy, TG produces an entropic force which drives the DW towards the hotter region [22, 23].

In our recent study [26], we demonstrated the TG induced DW dynamics in a uniaxial nanowire but the nanowire structure has a significant effect on DW dynamics under TG. Therefore, in this paper, we study DW dynamics along a biaxial and uniaxial nanowire under TG and present a comparison of the DW dynamics in the considered nanowires. We find that the DW propagates toward the hotter region in both nanowires. For the uniaxial nanowire, the DW propagates towards a hotter region, accompanying a rotational motion of the DW-plane around the easy axis. Both (propagation and rotational) speeds increase proportionately with the increase of TG. For the biaxial nanowire, DW also propagates in the hotter region with a significantly larger speed than the speed in the uniaxial nanowire. DW speed in biaxial nanowire initially increases with the TG. However, after certain TGs, the propagation speed decreases and afterwards, it shows an increasing trend again for the further increment of a TG, i.e., the so-called Walker breakdown phenomenon is observed. We also study the Gilbert damping (α) dependent DW dynamics and find that DW's both, linear and rotational speeds decrease with damping since α reduces the magnonic current. So, the above findings of DW dynamics in biaxial/uniaxial nanowire under TG may lead to realizing the spintronic (specially racetrack memory) devices.

2. Analytical Model and Method

We consider a uniaxial and biaxial ferromagnetic nanowire with a head-to-head DW at the centre along the x -axis (easy axis) of length L_x and cross-sectional area $L_y \times L_z$ as shown

*Corresponding author:

 torikul@phy.ku.ac.bd (M.T. Islam)

ORCID(s): 0000-0002-3846-4009 (M.T. Islam); 0000-0003-1723-6012 (J.M.T. Islam); 0000-0002-6742-2158 (M.A.S. Akanda); 0000-0002-7500-1572 (M.A.J. Pikul); 0000-0002-9933-9922 (F. Yesmin)

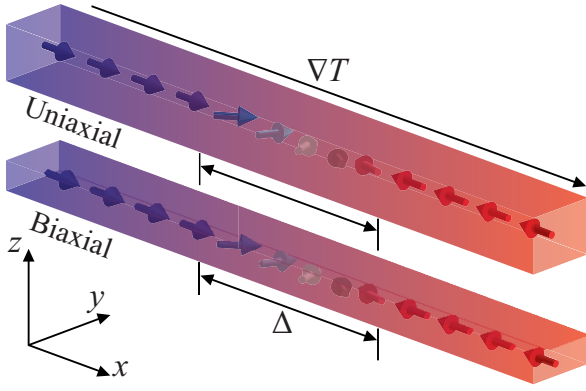


Figure 1: Schematic diagram of considered nanowires (Uniaxial and biaxial) with a head-to-head DW at the centre under the TG ∇T . The Blue (red) colour represents the colder (hotter) region of the sample.

in Fig.1. The DW width Δ is larger than the dimension of L_y , L_z but much smaller than L_x . The hard anisotropy of biaxial nanowire is given by $K_{\perp} = 1/2\mu_0 M_s^2(\mathcal{N}_y - \mathcal{N}_z)$ along z -direction with $\mathcal{N}_z \geq \mathcal{N}_y$, where \mathcal{N}_x , \mathcal{N}_y and \mathcal{N}_z are demagnetization factors. However, for uniaxial nanowire, $\mathcal{N}_z = \mathcal{N}_y$, i.e., $K_{\perp} = 0$. A TG as a driving force is applied along the nanowire. The applied highest temperature is far below the Curie temperature T_c . It is assumed that the saturation magnetization and exchange constant are temperature-independent. The magnetization dynamics is governed by the stochastic Landau-Lifshitz-Gilbert (sLLG) equation [27, 28],

$$\frac{d\mathbf{m}}{dt} = -\mathbf{m} \times (\mathbf{h}_{\text{eff}} + \mathbf{h}_{\text{th}}) + \alpha \mathbf{m} \times \frac{\partial \mathbf{m}}{\partial t}, \quad (1)$$

where $\mathbf{m} = \mathbf{M}/M_s$ and M_s are respectively the magnetization direction and the saturation magnetization. α is the Gilbert damping constant and t is the time measured in the units of $(|\gamma|M_s)^{-1}$ in which γ is the gyromagnetic ratio. $\mathbf{h}_{\text{eff}} = \frac{2A}{M_s} \sum_{\sigma} \frac{\partial \mathbf{m}}{\partial x_{\sigma}} + K_{\parallel} m_x \hat{\mathbf{x}} + \mathbf{h}_{\text{dipole}}$ is the effective field measured in the units of M_s , where A is the exchange stiffness constant, x_{σ} ($\sigma = 1, 2, 3$) denote Cartesian coordinates x, y, z , K_{\parallel} is the easy-axis anisotropy, and $\mathbf{h}_{\text{dipole}}$ is the dipolar field and \mathbf{h}_{th} is the thermal stochastic field.

The stochastic LLG equation is solved numerically by the micromagnetic simulation package MUMAX3 [29] in which we use adaptive Heun solver. The time step is chosen 10^{-14} s for the unit cell size $(2 \times 2 \times 2) \text{ nm}^3$ and 10^{-15} s for unit cell smaller than $(2 \times 2 \times 2) \text{ nm}^3$. The saturation magnetization $M_s = 8 \times 10^5 \text{ A/m}$ and exchange stiffness constant $A = 13 \times 10^{-12} \text{ J/m}$ are used to mimic permalloy in our simulations. The thermal field follows the Gaussian process characterized by following statistics

$$\begin{aligned} \langle h_{\text{th},ip}(t) \rangle &= 0, \\ \langle h_{\text{th},ip}(t) h_{\text{th},jq}(t + \Delta t) \rangle &= \frac{2k_B T_i \alpha_i}{\gamma M_s a^3} \delta_{ij} \delta_{pq} \delta(\Delta t) \end{aligned} \quad (2)$$

where i and j denote the micromagnetic cells, and p, q represent the Cartesian components of the thermal field. T_i and α_i

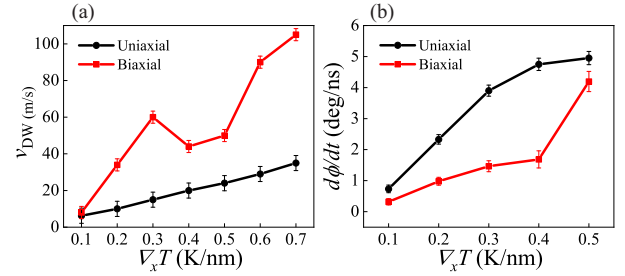


Figure 2: A comparison of DW dynamics under TG $\nabla_x T$ along biaxial ($1024 \times 30 \times 4 \text{ nm}^3$) and uniaxial ($1024 \times 4 \times 4 \text{ nm}^3$) nanowire. (a) Red and black lines represent the DW-linear speeds (v_{DW}) along biaxial and uniaxial nanowire respectively. (b) Black and red lines represent DW-plane's rotational speeds ($\frac{d\phi}{dt}$) along uniaxial and biaxial nanowire respectively.

are respectively temperature and the Gilbert damping at cell i , and a is the cell size. k_B is the Boltzmann constant [27]. The numerical results presented in this study are averaged over 15 random configurations.

3. Numerical Results

3.1. Thermal gradient dependent DW dynamics

In order to compare the DW dynamics (linear and DW-angular speeds) in the biaxial and uniaxial nanowires, 15 random trajectories of DW propagation are generated for each set of parameters and the TG. Then we take the statistical ensemble average to obtain the time dependent average DW position, and hence DW's linear (v_{DW}) and rotational ($d\phi/dt$) speeds are estimated. In both cases, the DWs propagate toward the hotter region. The comparison between DW's linear and rotational speeds in biaxial and uniaxial nanowires is shown in Fig. 2(a) and (b), respectively. In the uniaxial nanowire under TG, the DW moves toward the hotter regions accompanying the rotation of the DW plane around the symmetry/easy axis. DW speed proportionately increases with the TG. It is interesting to note that the DW linear speed (rotational speed) in the biaxial nanowire is significantly larger (smaller) than the DW linear speed (rotational speed) in the uniaxial nanowire. To explain the reason why the DW linear speed is larger in biaxial nanowire, one can look at the expression of hard anisotropy $K_{\perp} = 1/2\mu_0 M_s^2(\mathcal{N}_z - \mathcal{N}_y)$, say along z -direction for biaxial nanowire while $K_{\perp} = 0$ for uniaxial nanowire (since \mathcal{N}_z and \mathcal{N}_y are equal). This hard anisotropy contributes a polar torque (Γ_{θ}) along θ -direction [30] since Γ_{θ} is proportional to $(\mathcal{N}_z - \mathcal{N}_y)$.

After certain TG, the DW-linear speed (rotational speed) decreases (increases), which indicates the Walker breakdown phenomena. With the further increment of TG, both DW-linear and rotational speeds show increasing trends. After the Walker breakdown limit, the biaxial nanowire behaves like a uniaxial nanowire and the DW linear and rotational speeds increase similarly to the uniaxial nanowire. These DW dynamics can be explained by microscopic theory as stating that more magnons are populated in the hotter region

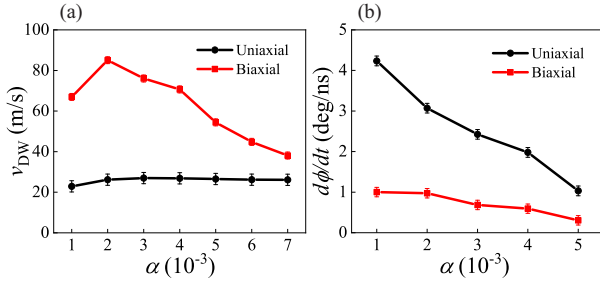


Figure 3: Damping (α) dependent (a) DW-linear speed represented by a red line (black line) along biaxial (uniaxial) nanowire. (b) DW-plane's rotational speed is represented by a red line (black line) along biaxial (uniaxial) nanowire.

and travel from the hotter to the colder region. During crossing the DW, the magnon exerts a magnonic torque on the DW by transferring spin angular momentum to the DW. In this way, magnons drive the DW toward the hotter region of the nanowire, opposite to the direction of the magnonic current [18, 19, 20, 21]. These findings are also consistent with the macroscopic theory [22, 23].

3.2. Damping dependent DW dynamics

Gilbert damping coefficient α is a crucial material parameter that has a significant effect on DW dynamics under TG. For fixed $\nabla_x T = 0.5$, we investigate the DW dynamics in biaxial and uniaxial nanowires of length $L_x = 1024$ nm. The obtained results of DW's linear and rotational speeds as a function of α are presented as in Fig. 3(a) and (b), respectively. In both nanowires, DW's speeds increase initially and then decrease with increasing α . Usually, the DW velocities should be decreased since the magnon propagation length decreases with damping. However, we observe that the DW speeds increase initially till a certain α and then decrease monotonically with α . To explain this observation, one can recall the basic physics of generating standing waves in the nanowire with fixed boundaries. If the length of the nanowire is not large enough and for lower damping, there is a probability to form the standing waves of some modes of spin-wave between the fixed boundaries. It is well known that the standing spin-wave does not carry any energy/spin angular momentum. Consequently, the energy transfer to the DW is decreased, i.e., DW velocity is decreased due to the decrement of the magnonic current. However, for larger α , the number of standing spin-waves decreases due to the reduction of propagation length of spin waves. Therefore, all modes of the spin-wave-spin current effectively interact with the DW, and hence the DW speeds increase. It is predicted that for the larger length of the nanowire, it may be observed that the DW speeds will decrease monotonically with α . The above statement would be justified in the next subsection. For a further increment of α , the magnon propagation length decreases with the damping, so the amount of spin angular momentum deposited on a DW should decrease. As a result, the DW propagation speed and DW-plane rotation speed decrease with α as shown in Fig. 3(a) and (b), respectively.

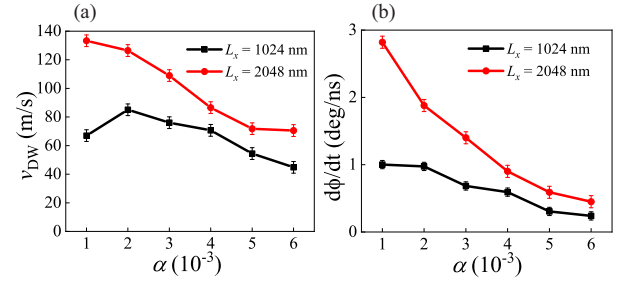


Figure 4: Damping α dependent (a) DW-linear speed represented by black line (red line) along biaxial nanowire of length $L_x = 1024$ nm ($L_x = 2048$ nm). (b) DW-plane's rotational speed represented by black line (red line) along biaxial nanowire of length $L_x = 1024$ nm ($L_x = 2048$ nm).

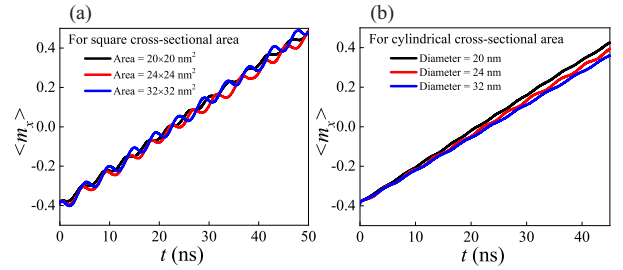


Figure 5: (a) Square and (b) cylindrical cross-sectional area dependent DW propagation along uniaxial nanowire.

3.3. Length dependent DW dynamics

Here, we present the behaviour of DW dynamics in two different lengths i.e., $L_x = 1024$ nm and $L_x = 2048$ nm of biaxial nanowire in Fig. 4(a) and (b) respectively, as a function of α (ranging from 0.001 to 0.006) for fixed TG $\nabla_x T = 0.5$ K/nm. Fig. 4(a) shows the DW linear velocity as a function of α corresponding to the nanowire lengths, $L_x = 1024$ nm (black) and $L_x = 2048$ nm (red). In Fig. 4(b), the black line and red line show the change of angular velocity as a function of α corresponding to the lengths $L_x = 1024$ nm and $L_x = 2048$ nm respectively. DW angular velocities also decrease with α . Since the magnons propagation length decreases with α [25], it reduces the number of magnons to pass through the DW, which leads to the reduction of DW velocity proportionately. It is noted that for smaller $L_x = 1024$ nm (Fig. 4(a)), the DW speed is lower for $\alpha = 0.001$, and it gradually increases and then monotonically decreases. Interestingly, such behaviour disappears with the increase of length, and for the length $L_x = 2048$ nm and the DW velocities show decreasing trend monotonically. The reason for observing such behaviour has been discussed above for shorter $L_x = 1024$ nm. Here we mention again shortly that for lower damping, the magnon propagation length is larger. If the length of the sample size is not large enough, then there is a probability of forming the standing waves of some modes between the fixed boundaries. Consequently, the energy transfer through the DW is decreased, i.e., DW velocity is decreased because of the reduction of the magnonic current.

3.4. Cross-sectional area dependent DW dynamics

The cross-sectional area of the nanowire has an influence on the DW dynamics. Fig. 5(a) and (b) show the DW dynamics in uniaxial nanowires of square and cylindrical cross-sectional area, respectively. For the nanowire with square cross-sectional area, it is observed that the DW propagates towards the hotter region with oscillatory or wavy nature. For larger cross-sectional area (32×32 nm²), the oscillation amplitude is larger. As we know from previous observation that the DW-plane rotates during propagation in the uniaxial nanowire. Thus the spins of DW experience asymmetric shape anisotropy during rotation as it faces the easy and hard axis anisotropy successively. When the DW faces hard anisotropy, its propagation speed increases and vice-versa. So the DW propagates with wavy nature. This wavy nature of DW propagation decreases in the sample of cylindrical cross-section as shown in Fig. 5(b). The reason is that, in the sample of cylindrical cross-section, the DW experiences almost symmetric shape anisotropy. Fig. 5(b) shows still small wavy nature propagation in the sample of cylindrical cross-sectional area because it is technically difficult to simulate the perfect cylindrical cross-section.

4. Discussions and Conclusions

In this study, we investigate the DW dynamics in uniaxial and biaxial nanowires under TG. We found that the DW propagates toward the hotter region in both nanowires. For the uniaxial nanowire, the DW propagates towards a hotter region, accompanying a rotational motion of the DW-plane around the easy axis. Both (propagation and rotational) speeds increase proportionately with the increase of TG. For biaxial nanowire, DW also propagates in the hotter region, and DW propagation speed is significantly larger than the speed in the uniaxial nanowire. DW speed in biaxial nanowire initially increases with the TG. But after certain TGs, the propagation speed decreases and afterwards, it shows an increasing trend again for the further increment of a TG, i.e., the so-called Walker breakdown phenomenon is observed. We also study the Gilbert damping α dependent DW dynamics and found that DW's both linear and rotational speeds decrease with damping since α reduces the magnonic current. In this study, we also examined the length and cross-sectional area dependent DW dynamics with damping coefficient. We found that it is required to optimize the damping coefficient with the nanowire structure to obtain the efficient DW speed under TG. Therefore the above findings of DW dynamics in biaxial/uniaxial nanowire under TG may might be useful for the fundamental interests and applications in spintronic devices.

Acknowledgments

This research acknowledges Khulna University Research Cell (Grant No. KU/RC-04/2000-158), Khulna, Bangladesh.

References

- [1] S. S. Parkin, M. Hayashi, L. Thomas, Magnetic domain-wall racetrack memory, *Science* 320 (5873) (2008) 190–194.
- [2] D. A. Allwood, G. Xiong, C. Faulkner, D. Atkinson, D. Petit, R. Cowburn, Magnetic domain-wall logic, *Science* 309 (5741) (2005) 1688–1692.
- [3] X. Wang, P. Yan, J. Lu, C. He, Magnetic field driven domain-wall propagation in magnetic nanowires, *Annals of Physics* 324 (8) (2009) 1815–1820.
- [4] X. Wang, P. Yan, J. Lu, High-field domain wall propagation velocity in magnetic nanowires, *EPL (Europhysics Letters)* 86 (6) (2009) 67001.
- [5] D. Atkinson, D. A. Allwood, G. Xiong, M. D. Cooke, C. C. Faulkner, R. P. Cowburn, Magnetic domain-wall dynamics in a submicrometre ferromagnetic structure, *Nature materials* 2 (2) (2003) 85–87.
- [6] G. S. Beach, C. Nistor, C. Knutson, M. Tsoi, J. L. Erskine, Dynamics of field-driven domain-wall propagation in ferromagnetic nanowires, *Nature materials* 4 (10) (2005) 741–744.
- [7] M. Hayashi, L. Thomas, Y. B. Bazaliy, C. Rettner, R. Moriya, X. Jiang, S. Parkin, Influence of current on field-driven domain wall motion in permalloy nanowires from time resolved measurements of anisotropic magnetoresistance, *Physical Review Letters* 96 (19) (2006) 197207.
- [8] L. Berger, Emission of spin waves by a magnetic multilayer traversed by a current, *Physical Review B* 54 (13) (1996) 9353.
- [9] J. C. Slonczewski, Current-driven excitation of magnetic multilayers, *Journal of Magnetism and Magnetic Materials* 159 (1-2) (1996) L1–L7.
- [10] S. Zhang, Z. Li, Roles of nonequilibrium conduction electrons on the magnetization dynamics of ferromagnets, *Physical review letters* 93 (12) (2004) 127204.
- [11] G. Tatara, H. Kohno, Theory of current-driven domain wall motion: Spin transfer versus momentum transfer, *Physical review letters* 92 (8) (2004) 086601.
- [12] A. Yamaguchi, T. Ono, S. Nasu, K. Miyake, K. Mibu, T. Shinjo, Real-space observation of current-driven domain wall motion in submicron magnetic wires, *Physical review letters* 92 (7) (2004) 077205.
- [13] A. Yamaguchi, A. Hirohata, T. Ono, H. Miyajima, Temperature estimation in a ferromagnetic Fe-Ni nanowire involving a current-driven domain wall motion, *Journal of Physics: Condensed Matter* 24 (2) (2011) 024201.
- [14] G. E. Bauer, E. Saitoh, B. J. Van Wees, Spin caloritronics, *Nature materials* 11 (5) (2012) 391–399.
- [15] W. Jiang, P. Upadhyaya, Y. Fan, J. Zhao, M. Wang, L.-T. Chang, M. Lang, K. L. Wong, M. Lewis, Y.-T. Lin, et al., Direct imaging of thermally driven domain wall motion in magnetic insulators, *Physical review letters* 110 (17) (2013) 177202.
- [16] X. Wang, P. Yan, X. Wang, Magnonic spin-transfer torque and domain wall propagation, *IEEE transactions on magnetics* 48 (11) (2012) 4074–4076.
- [17] C. Safranski, I. Barsukov, H. K. Lee, T. Schneider, A. Jara, A. Smith, H. Chang, K. Lenz, J. Lindner, Y. Tserkovnyak, et al., Spin caloritronic nano-oscillator, *Nature communications* 8 (1) (2017) 1–7.
- [18] P. Yan, X. Wang, X. Wang, All-magnonic spin-transfer torque and domain wall propagation, *Physical review letters* 107 (17) (2011) 177207.
- [19] A. A. Kovalev, Y. Tserkovnyak, Thermomagnonic spin transfer and peltier effects in insulating magnets, *EPL (Europhysics Letters)* 97 (6) (2012) 67002.
- [20] X. G. Wang, G. H. Guo, Y. Z. Nie, G. F. Zhang, Z. X. Li, Domain wall motion induced by the magnonic spin current, *Physical Review B* 86 (5) (2012) 054445.
- [21] P. Yan, Y. Cao, J. Sinova, Thermodynamic magnon recoil for domain wall motion, *Physical Review B* 92 (10) (2015) 100408.
- [22] F. Schlickeiser, U. Ritzmann, D. Hinzke, U. Nowak, Role of entropy in domain wall motion in thermal gradients, *Physical review letters* 113 (9) (2014) 097201.
- [23] S. Etesami, L. Chotorlishvili, A. Sukhov, J. Berakdar, Longitudinal

spin current induced by a temperature gradient in a ferromagnetic insulator, *Physical Review B* 90 (1) (2014) 014410.

- [24] X. Wang, X. Wang, Thermodynamic theory for thermal-gradient-driven domain-wall motion, *Physical Review B* 90 (1) (2014) 014414.
- [25] D. Hinzke, U. Nowak, Domain wall motion by the magnonic spin seebeck effect, *Physical review letters* 107 (2) (2011) 027205.
- [26] M. T. Islam, X. Wang, X. Wang, Thermal gradient driven domain wall dynamics, *Journal of Physics: Condensed Matter* 31 (45) (2019) 455701.
- [27] W. F. Brown Jr, Thermal fluctuations of a single-domain particle, *Physical review* 130 (5) (1963) 1677.
- [28] T. L. Gilbert, A phenomenological theory of damping in ferromagnetic materials, *IEEE transactions on magnetics* 40 (6) (2004) 3443–3449.
- [29] A. Vansteenkiste, J. Leliaert, M. Dvornik, M. Helsen, F. Garcia-Sanchez, B. Van Waeyenberge, The design and verification of mumax3, *AIP advances* 4 (10) (2014) 107133.
- [30] A. Mougin, M. Cormier, J. Adam, P. Metaxas, J. Ferré, Domain wall mobility, stability and walker breakdown in magnetic nanowires, *EPL (Europhysics Letters)* 78 (5) (2007) 57007.